Electronic Supplementary Information

MS/MS Fragmentation-guided search of TMG-chitooligomycins and their structure-activity relationship in specific *β*-*N*-acetylglucosaminidase inhibition

Hirokazu Usuki,[ab] Yukihiro Yamamoto,[a] Yuya Kumagai,[a] Teruhiko Nitoda,[c] Hiroshi Kanzaki,[c] and Tadashi Hatanaka*[a]

[a] *Okayama Prefectural Technology Center for Agriculture, Forestry and Fisheries, Research Institute for Biological Sciences (RIBS), 7549-1 Kibichuo-cho, Kaga-gun, Okayama 716-1241, Japan, Fax: +81 866 56 9454; Tel: +81 866 56 9452, E-mail: hatanaka@bio-ribs.com*

[b] *Research Fellow of the Japan Society for the Promotion of Science (JSPS), Japan*

[c] *Laboratory of Bioresources Chemistry, The Graduate School of Natural Science and Technology, Okayama University, Okayama 700-8530, Japan*

Contents

Section-1: LC/MRM analysis.

1-1: For isolation of 2 and 3 (Fig. 3).

At each step of purification, a portion of the obtained fractions was analyzed by subsequent LC/MRM analysis using a Hypercarb column (2.1 x 100 mm). The mobile phase was water containing 0.1 % (v/v) HCOOH (A) and MeOH containing 0.1 % (v/v) HCOOH (B) at a flow rate of 0.3 ml/ min. The LC conditions were 100% A during 0–2 min, linearly increasing from 0–70 % B during 2–10 min, and 70% B during 10–15min.

1-2: For component sugar analysis.

Authentic $_{D}$-Glc and $_{D}$-GlcNAc were subjected to the butanolysis and *N*-acetylation procedures as described in the main text. The obtained solution containing the corresponding butylglycoside was dried and subsequently dissolved in H_2O. The solution was subjected to MS/MS analysis to construct specific MRM channels. The channels were used for the selective detention of corresponding butylglycosides. The column used was the same as in section 1-1. In this analysis, the mobile phase was water containing 0.1 % (v/v) HCOOH (A) and MeOH containing 0.1 % (v/v) HCOOH (B) at a flow rate of 0.3 ml/ min. The LC conditions were 100% A during 0–2 min, linearly increasing from 0–70 % B during 2–20 min, and 70% B during 20–24min. The analysis system was sufficient to distinguish the $_{D}$- and $_{L}$- forms of Glc as shown in Fig. S1.

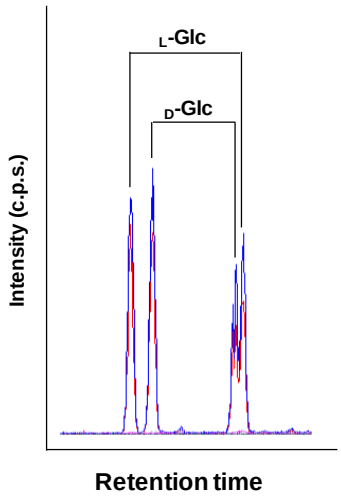

Fig. S1 Separation of (R)-2-butylglycoside of $_{D/L}$-Glc

1-3: For analysis of chitinase treated 1, 2, and 3 (Fig. 5), and the time course experiment (Fig. 6).

The column used was the same as in section 1-1. In this analysis, the mobile phase was water containing 0.1 % (v/v) HCOOH (A) and MeOH containing 0.1 % (v/v) HCOOH (B) at a flow rate of 0.3 ml/ min. The LC conditions were 100% A during 0–1 min, linearly increasing from 0–70 % B during 1–10 min, and 70% B during 10–14min.

Section-2: MS/MS spectra.

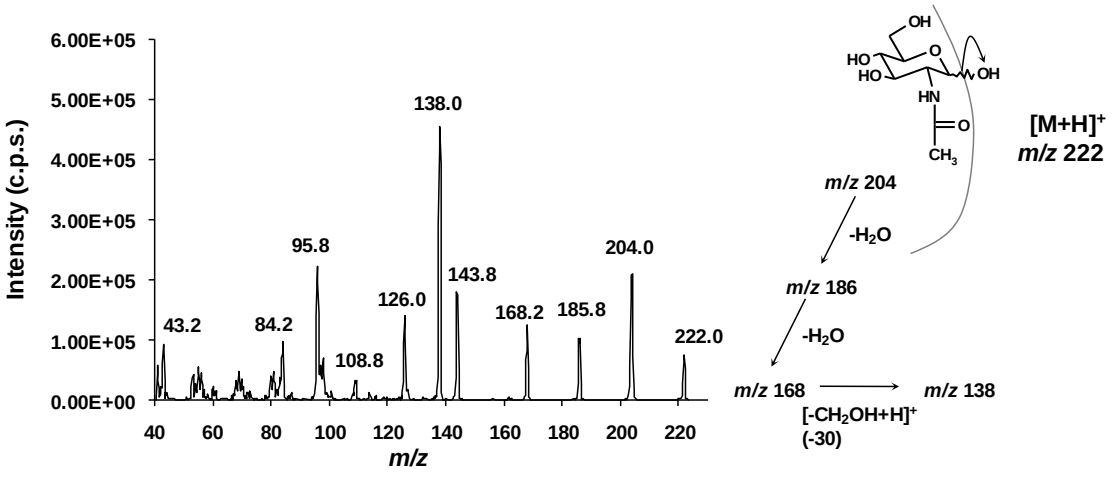

Fig. S2 MS/MS spectrum of GlcNAc

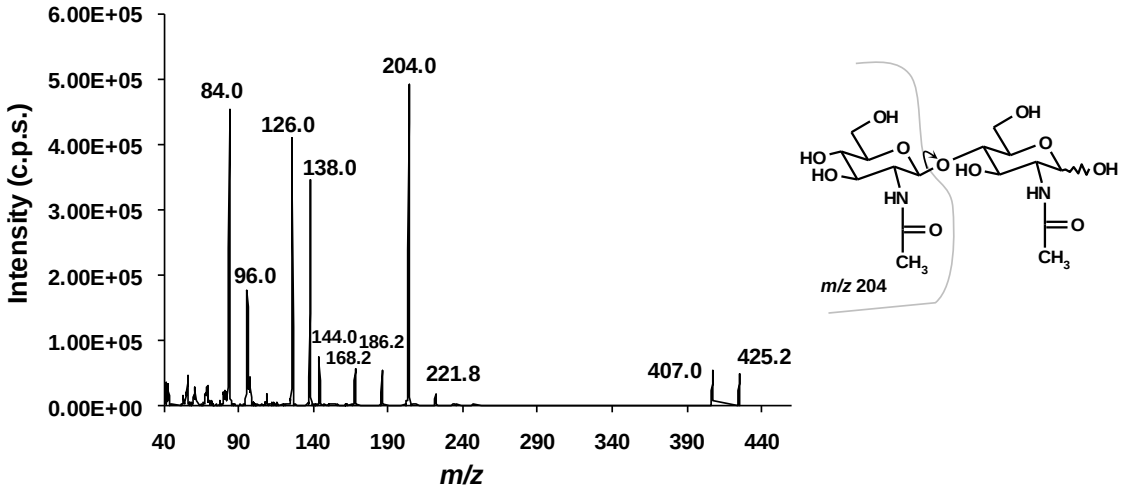

Fig. S3 MS/MS spectrum of $GlcNAc_2$

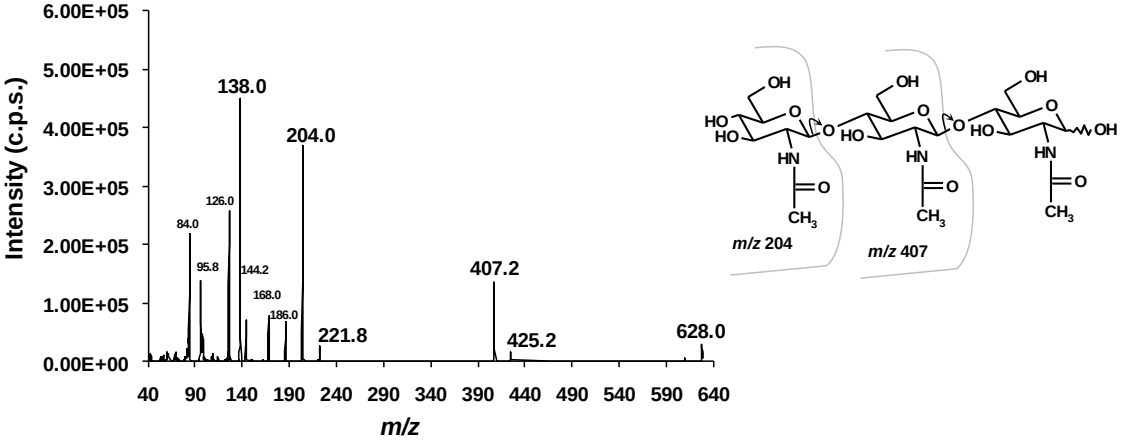

Fig. S4 MS/MS spectrum of $GlcNAc_3$

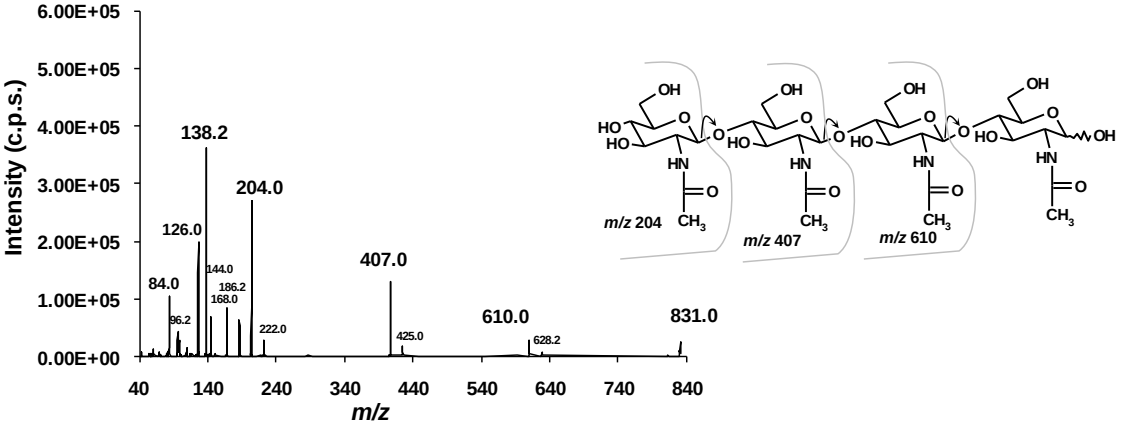

Fig. S5 MS/MS spectrum of $GlcNAc_4$

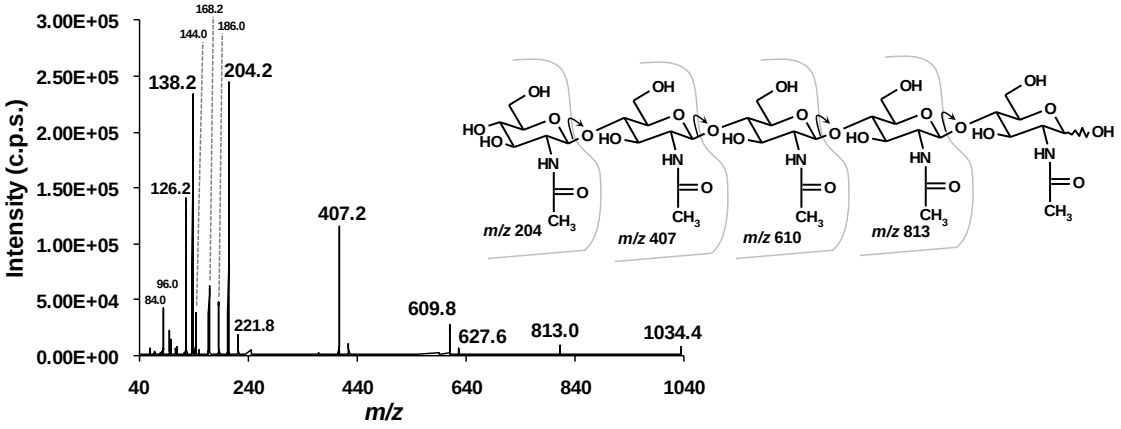

Fig. S6 MS/MS spectrum of $GlcNAc_5$

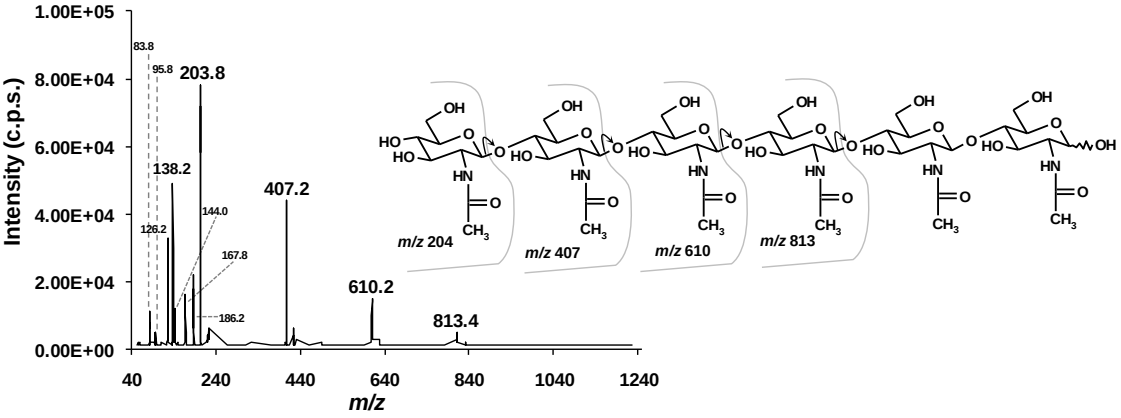

Fig. S7 MS/MS spectrum of $GlcNAc_6$

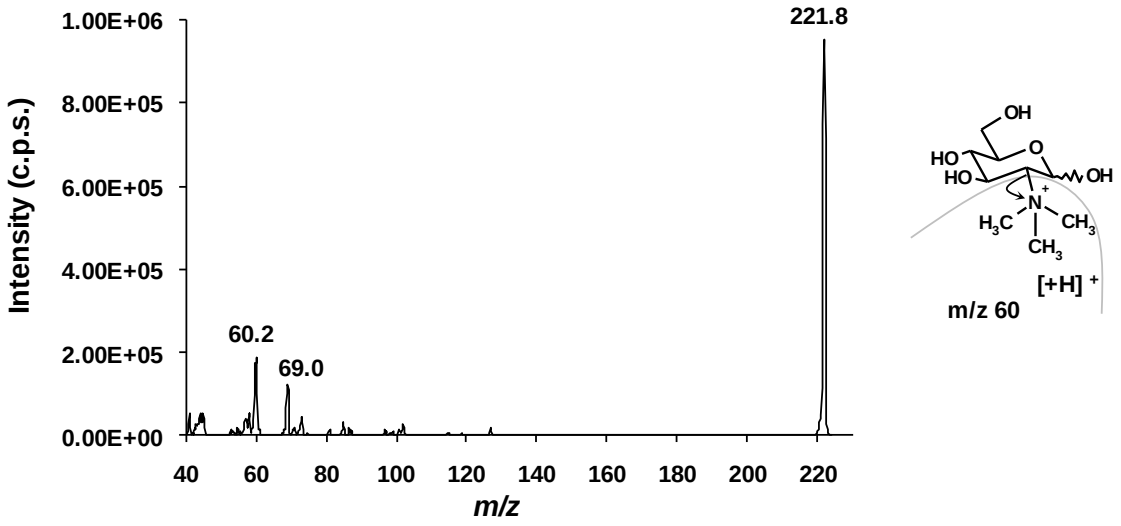

Fig. S8 MS/MS spectrum of TMG

Section-3: Enzymatic characteristics of SCO2758 and SCO2786.

3-1: SDA-PAGE analyses.

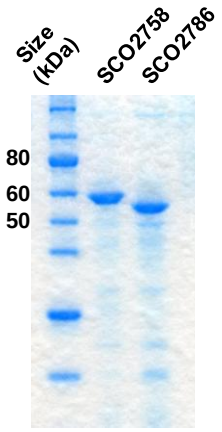

Fig. S9 SDS-PAGE of SCO2758 and SCO2786

3-2: Enzymatic properties of SCO2758 and SCO2786.

Table S1. Enzymatic properties of SCO 2758 and SCO2786

Properties	SCO2758	SCO2786
Family	GH3	GH20
Optimum pH[a]	pH 6.5	pH 4.4
V_{max}(μmol/min/mg) [b]	0.423	44.9
K_m (mM) [b]	72.7	79.3

[a] Toward 0.5 mM *p*NP-GlcNAc in 50 mM citrate-phosphate-borate buffer at 37°C for 60 min. [b] Toward *p*NP-GlcNAc.

Section-4: Lineweaver-Burk plots of 2 and 3.

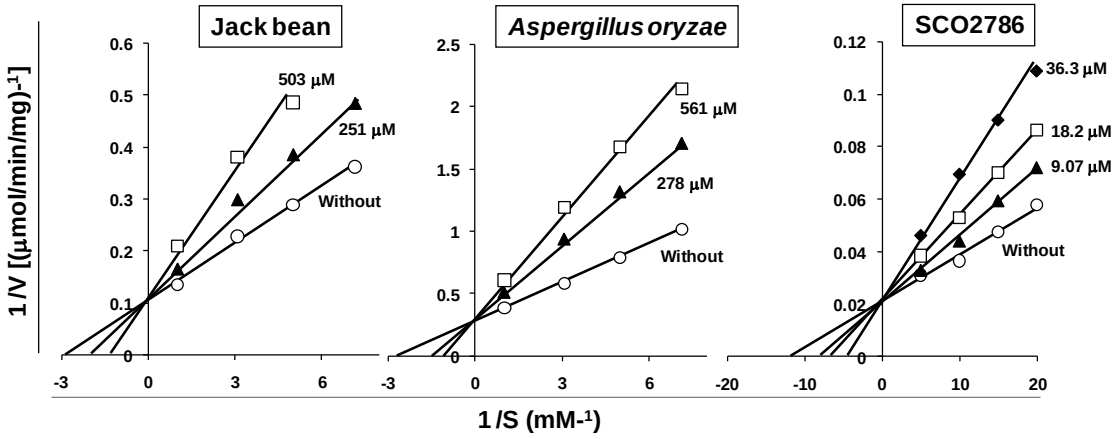

Fig. S10 Lineweaver-Burk plots of TMG-chitomonomycin(3)

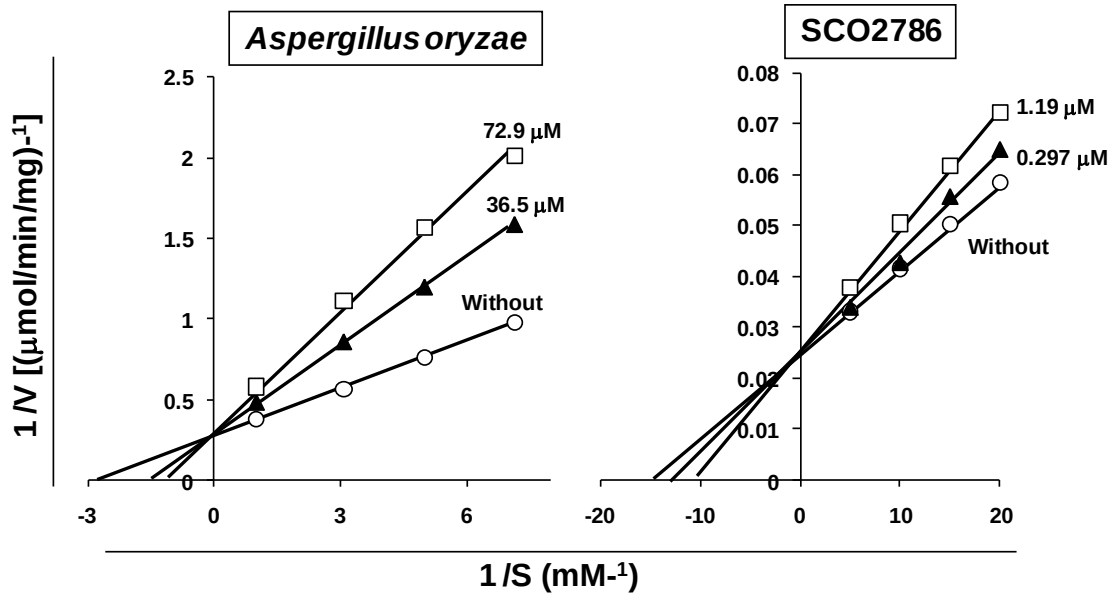

Fig. S11 Lineweaver-Burk plots of TMG-chitobiomycin(2)

Section-5: NMR data of 2and 3.

Table S2. ^{1}H-and ^{13}C-NMR data of TMG-chitomonomycin (**3**)

Sugar A (TMG)	Anomer of reducing end GlcNAc	δ_H (mult. *J* in Hz) 600 MHz	δ_C 150 MHz
1	α	5.42 (d, 3.8)	96.580
	β	5.41 (d, 4.1)	96.370
2	α	3.637 (dd, 3.8,7.2)	79.030
	β	3.637 (dd, 4.1,7.2)	78.910
3	α	4.04 (dd, 7.2, 8.8)	69.990
	β	4.04 (dd, 7.2, 8.8)	70.020
4	α	3.89 (dd, 8.8, 10.1)	69.300
	β	3.89 (dd, 8.8, 10.1)	69.400
5	α	3.67(ddd, 2.6, 6.1, 10.1)	77.120
	β	3.67(ddd, 2.6, 6.1, 10.1)	77.090
6a	α	3.78(dd, 6.1, 13.0)	61.120
	β	3.78(dd, 6.1, 13.0)	61.190
6b	α	3.84 (dd, 2.6, 13.0)	61.120
	β	3.90 (dd, 2.6, 13.0)	61.190
7-9	α	3.322(s)	54.38
	β	3.318(s)	54.38
Sugar B (reducing end GlcNAc)			
1	α	5.19 (d, 3.5)	91.35
	β	4.71 (d, 8.5)	95.55
2	α	3.92 (dd, 3.5, 10.5)	54.99
	β	3.70 (dd, 8.5, 10.0)	57.75
3	α	4.03 (dd, 9.3,10.5)	69.32
	β	3.68 (dd, 9.4, 10.0)	75.19
4	α	3.88 (overlapped)	77.68
	β	3.90 (overlapped)	78.15
5	α	4.08 (overlapped)	70.71
	β	3.84 (overlapped)	72.11
6a	α	3.80 (dd,6.2, 12.2)	62.04
	β	3.80 (dd,6.2, 12.2)	61.98
6b	α	3.89 (overlapped)	62.04
	β	3.89 (overlapped)	61.98
7	α	-	175.26[a]
	β	-	175.49[a]
8	α	2.046 (s)	22.55[a]
	β	2.044 (s)	22.83[b]

[a,b] Could be interchanged with one another.

Table S3. ^{1}H-and ^{13}C-NMR data of TMG-chitobiomycin (**2**)

Sugar A (TMG)	Anomer of reducing end GlcNAc	δ_H (mult. *J* in Hz) 600 MHz	δ_C 150 MHz
1	-	5.41(d, 3.8)	96.400
2	-	3.63(dd, 3.8, 8.1)	78.940
3	-	4.04(dd, 8.1, 8.1)	70.010
4	-	3.88(dd, 8.1, 8.1)	69.360
5	-	3.66 (ddd, 2.1, 5.9, 8.1)	77.120
6a	-	3.78(dd, 5.9, 12.4)	61.000
6b	-	3.91(dd, 2.1, 12.4)	-
7-9	-	3.32(s)	54.41
Sugar B			
1	α	4.59(d, 8.5)	101.99
	β	4.58(d, 8.2)	101.99
2	α	3.80 (overlapped)	56.66
	β	3.78 (overlapped)	56.62
3	-	3.72 (overlapped)	75.11
4	-	3.89 (overlapped)	77.53
5	-	3.88 (overlapped)	70.63
6a	-	3.78 (dd, 5.9, 12.4)	61.97
6b	-	3.88 (dd, 2.2, 12.6)	
7	α	-	175.41[a]
	β	-	175.35[a]
8	α	2.07(s)	22.83[b]
Sugar C (reducing end GlcNAc)			
1	α	5.18(d, 2.4)	91.13
	β	4.69(d, 7.9)	95.47
2	α	3.88(overlapped)	54.31
	β	3.68(overlapped)	56.78
3	α	3.88(overlapped)	69.96
	β	3.68(overlapped)	73.18
4	α	3.62,(overlapped)	80.31
	β	3.62,(overlapped)	79.86
5	α	3.89(overlapped)	71.71
	β	3.51(ddd, 2.1, 5.3, 9.7)	75.21
6a	α	3.78(dd, 5.9, 12.4)	60.76
	β	3.65(dd, 5.3, 12.4)	60.64
6b	α	3.92(overlapped)	-
	β	3.83(dd, 2.1, 12.4)	-
7	α	-	175.35[a]
	β	-	175.15[a]
8	α	2.033(s)	22.77[b]
	β	2.031(s)	22.54[b]

[a,b] Could be interchanged with one another.

^{1}H, Compound (2)

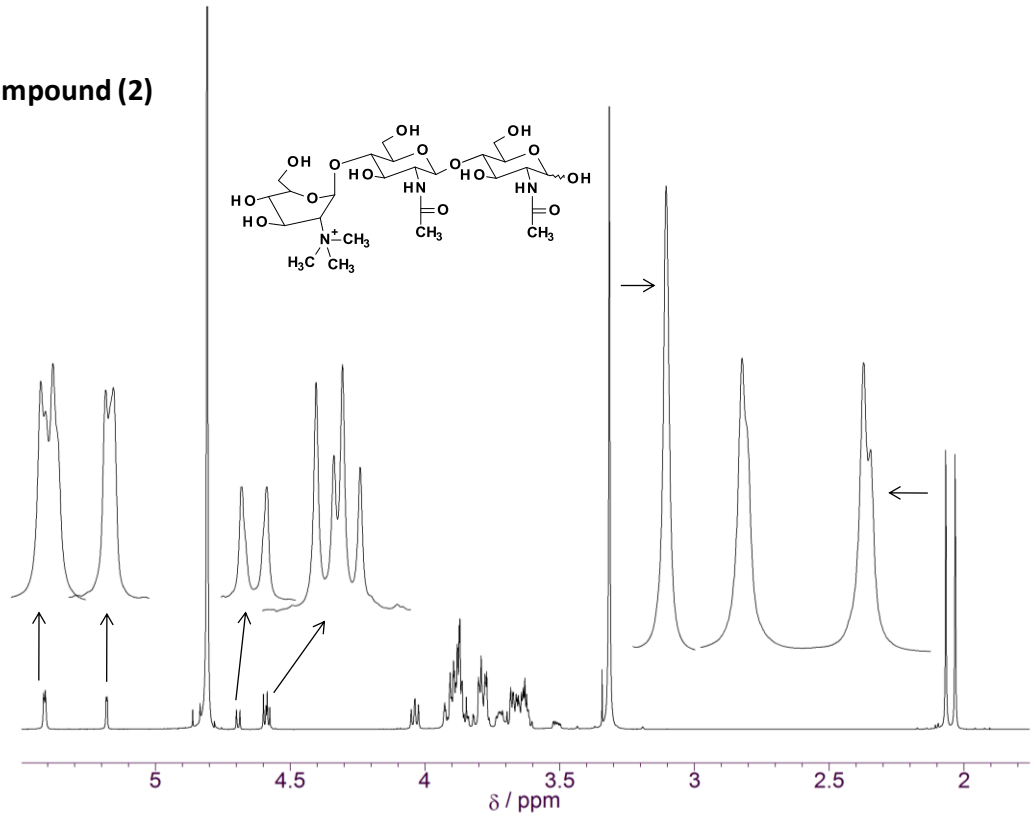

^{13}C, Compound (2)

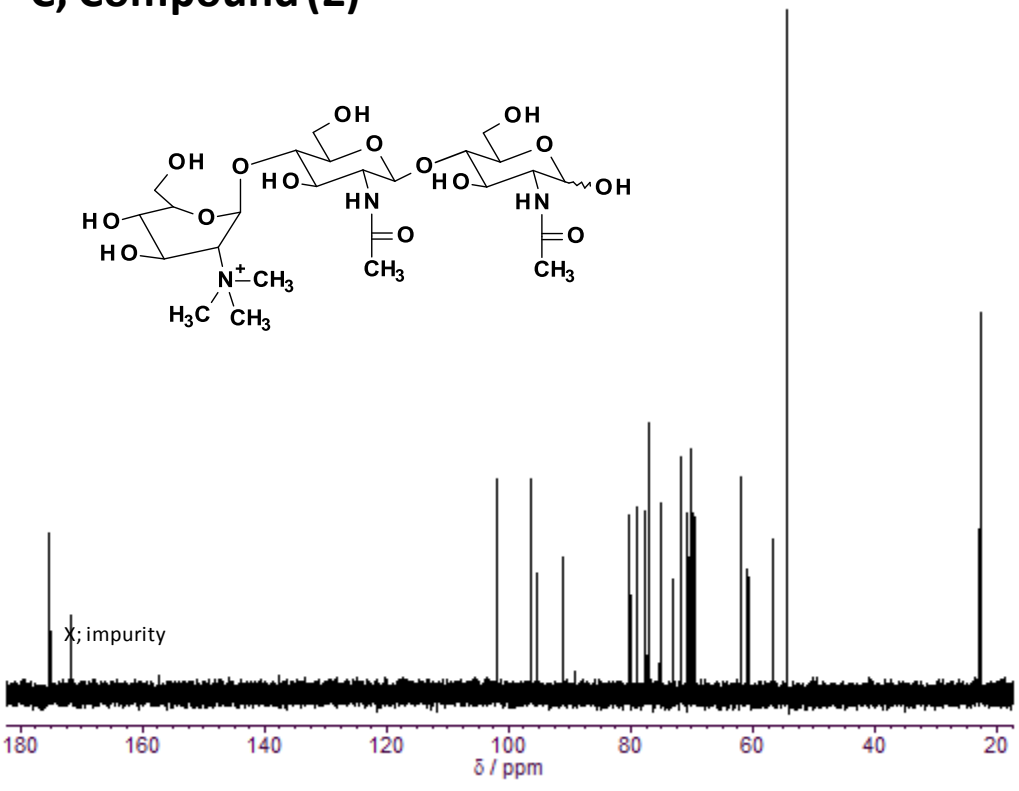

COSY, Compound (2)

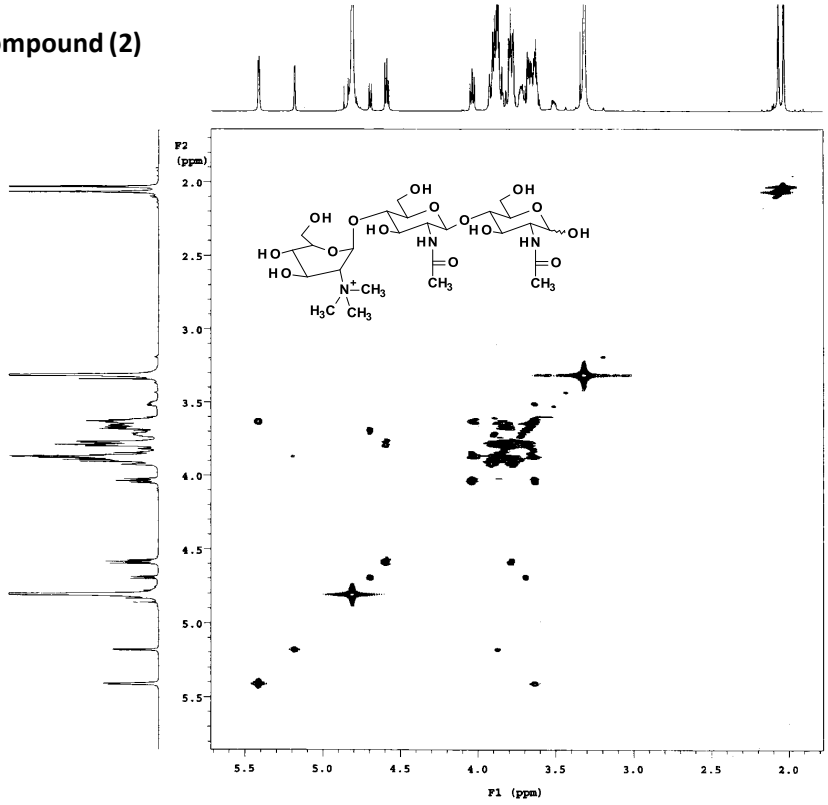

HSQC, Compound (2)

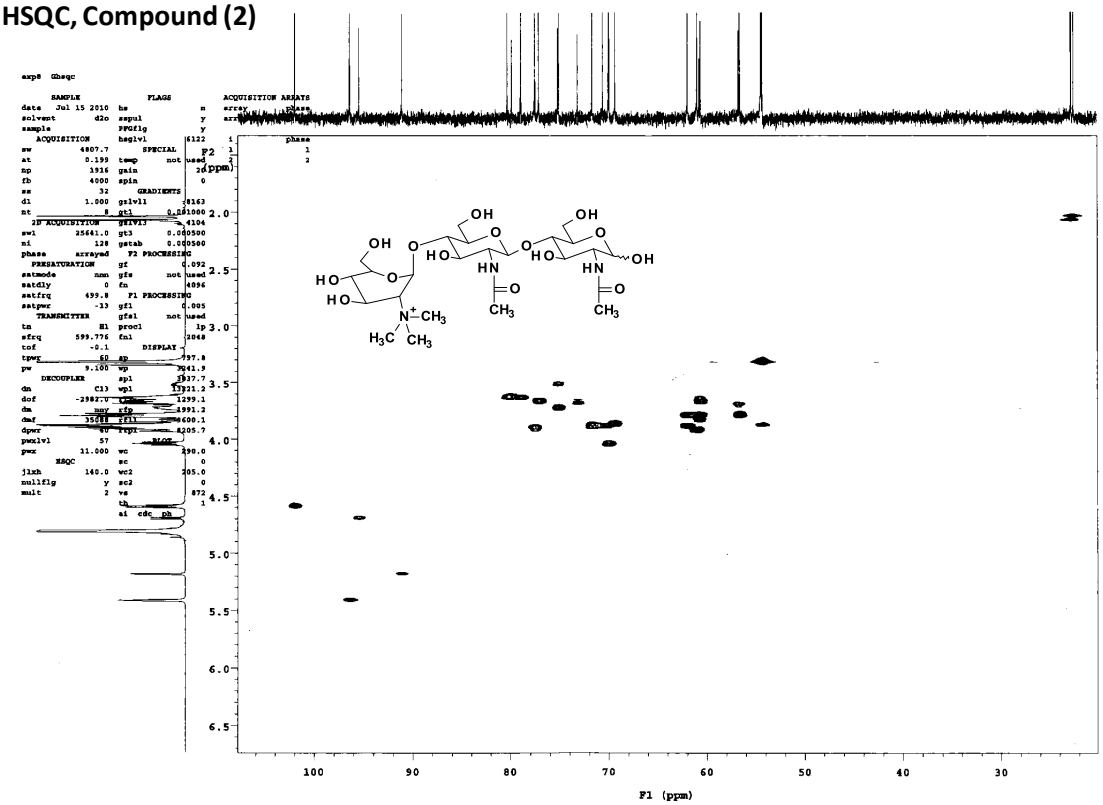

HMBC, Compound (2)

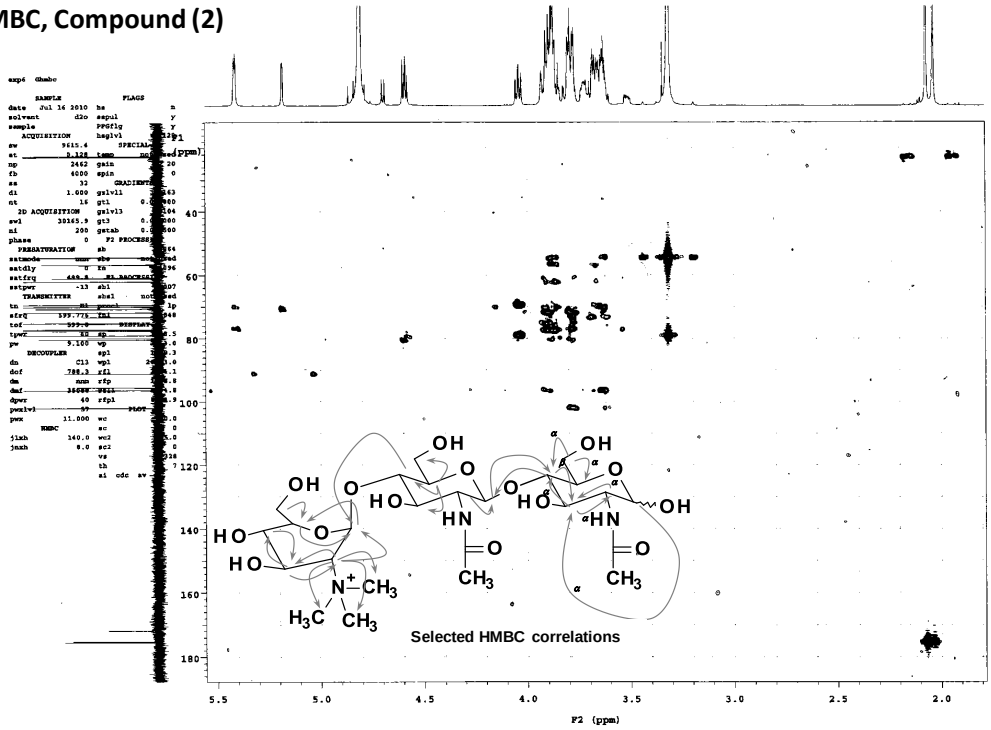

NOESY, Compound (2)

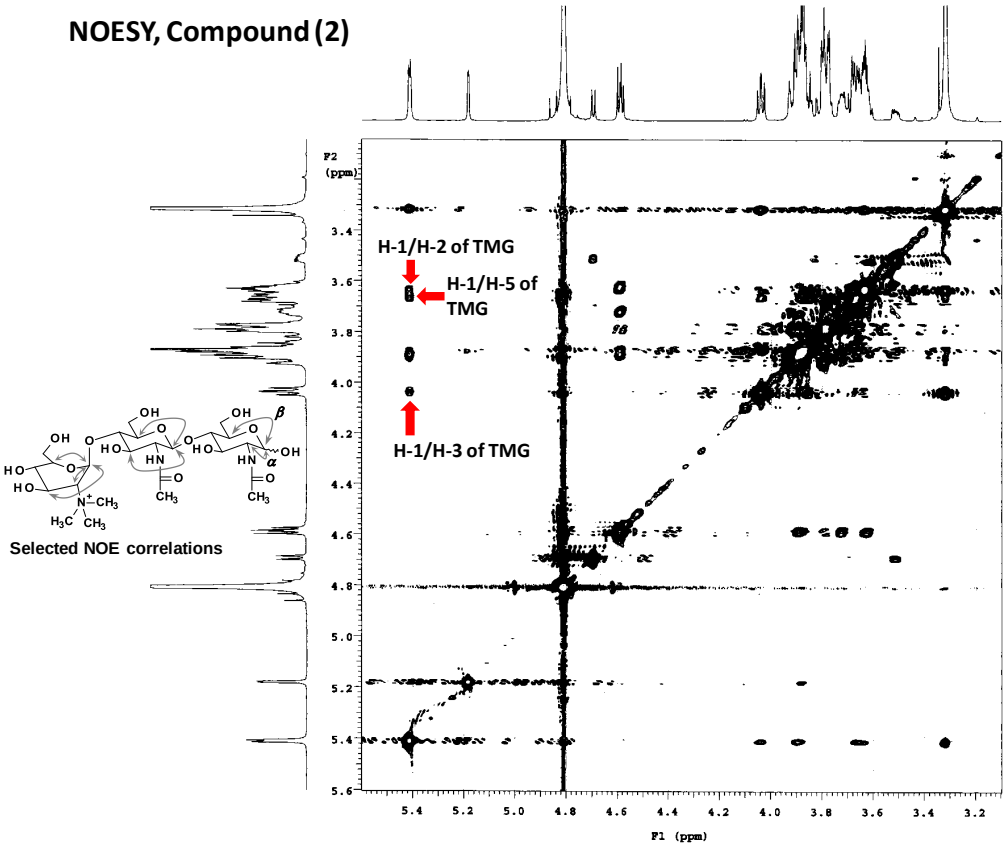

^{1}H, Compound (3)

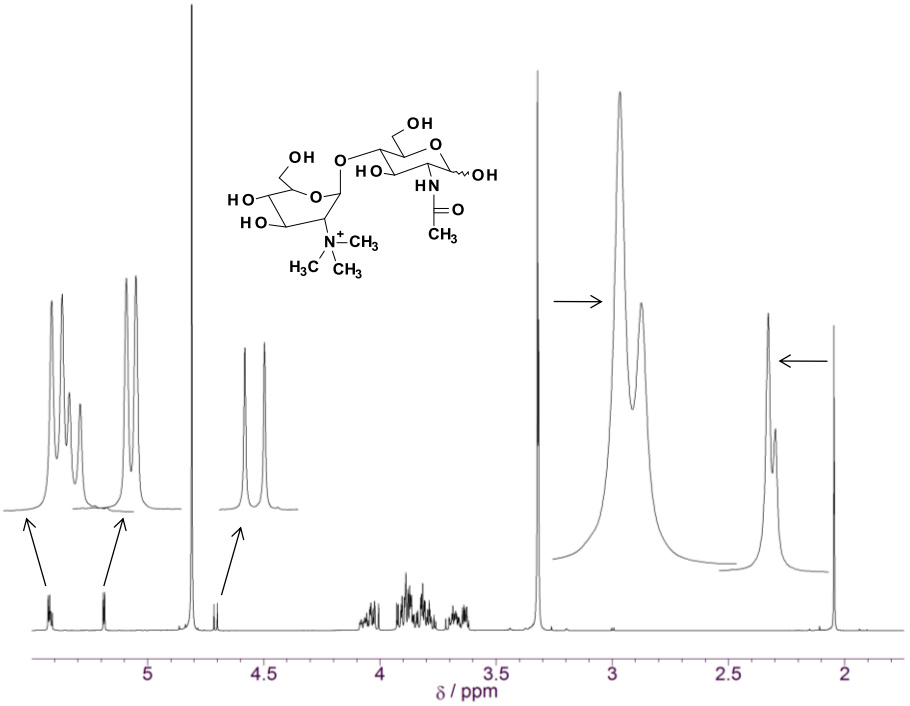

^{13}C, Compound (3)

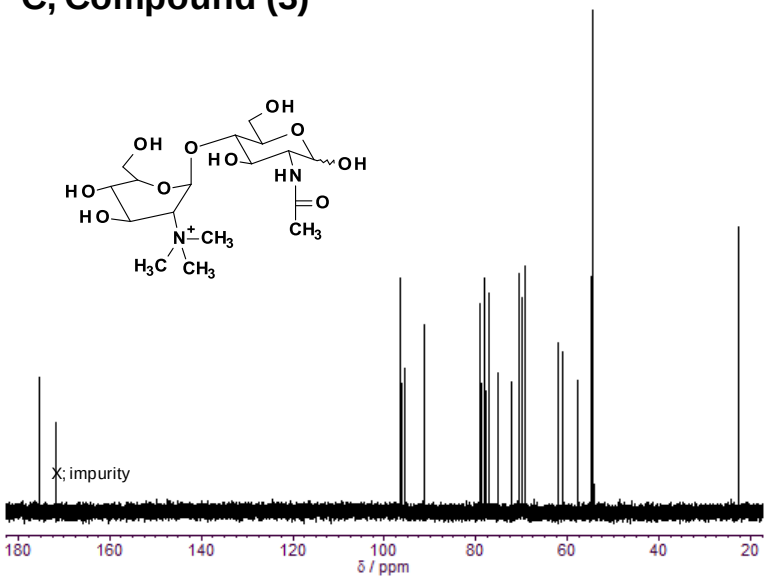

COSY, Compound (3)

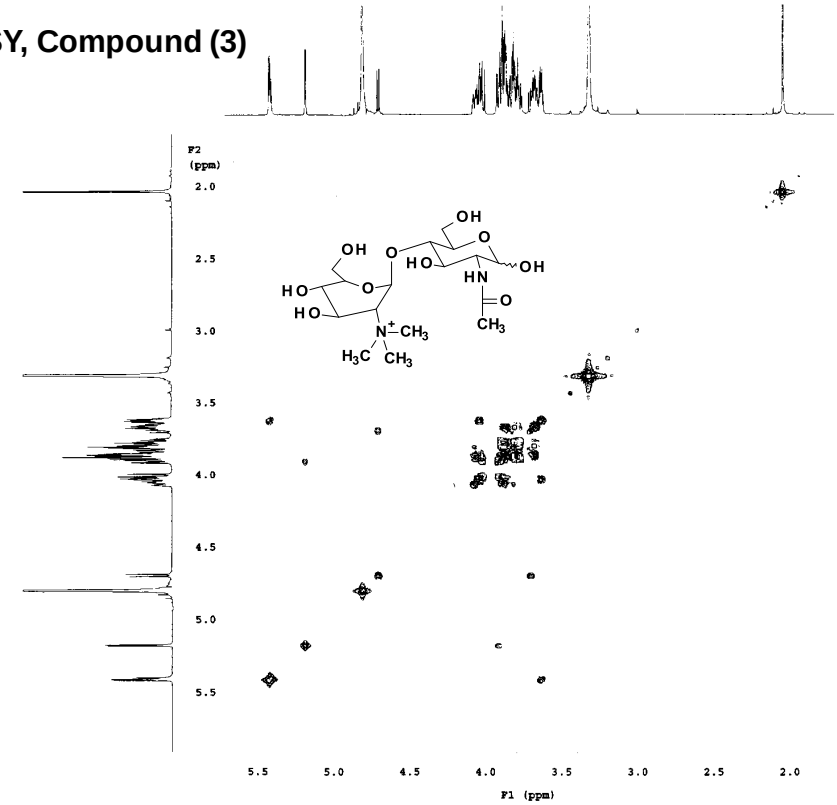

HSQC, Compound (3)

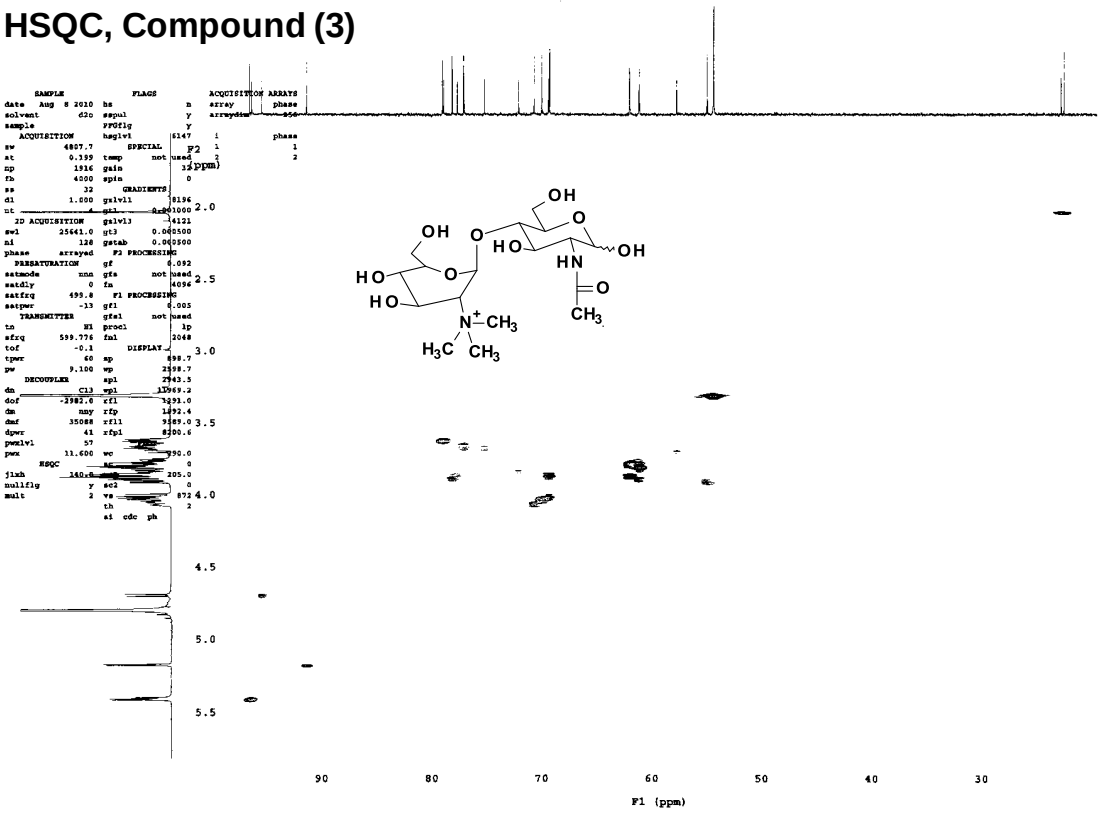

HMBC, Compound (3)

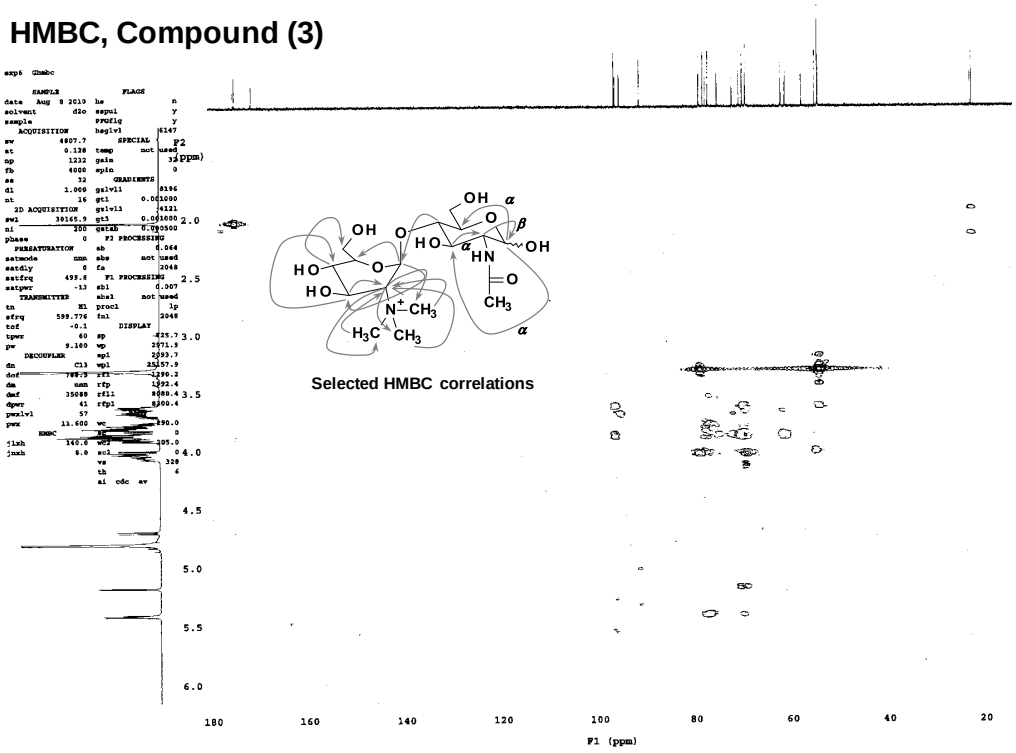

NOESY, Compound (3)

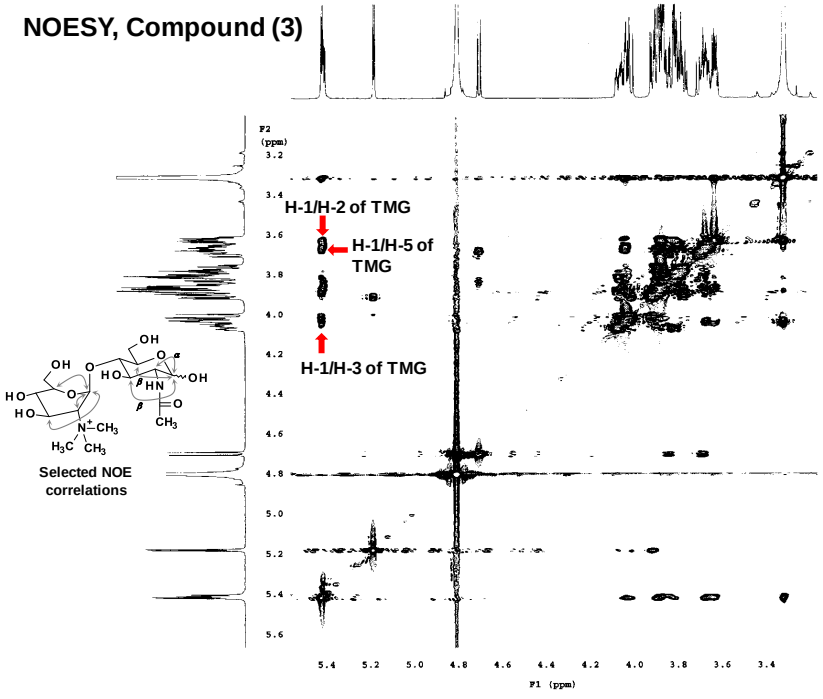

Section-6: NOESY spectra of free TMG and its $^4C_1$ conformation

A free $_D$-TMG was synthesized as described in our previous study[1]. The synthesized $_D$-TMG was subjected to the ^{1}H-NMR and NOESY experiments in D_2O to clarify its conformation. Assignment of ^{1}H-NMR signals was shown in the inner table of Fig.S12. The *J*-values of the observed ^{1}H signals and the NOE correlations of H-1/H-2 and H-3/H-5 indicated that free $_D$-TMG form a typical $^4C_1$ conformation with an α anomeric configuration.

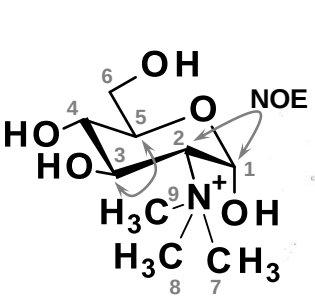

$_D$-*N,N,N*-trimethyl-glucosaminium

	δ_H (mult. *J in Hz*) 600 MHz
1	5.69 (d, 3.1)
2	3.57(dd, 3.1, 11.1)
3	4.29 (dd, 9.1, 11.1)
4	3.54 (dd, 9.1, 10.2)
5	3.91 (ddd, 2.1, 5.1, 10.2)
6a	3.78 (dd, 2.2, 12.4)
6b	3.85 (dd, 5.1, 12.4)
7-9	3.35 (s)

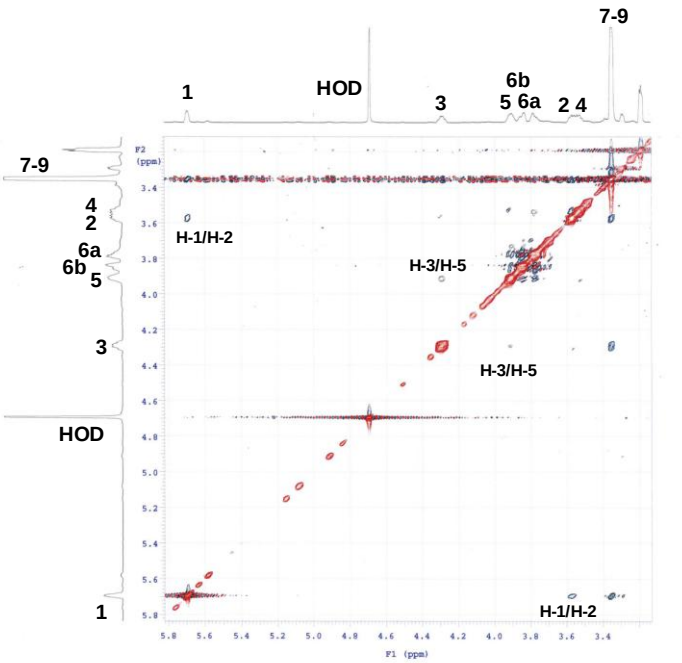

Fig.S12 NOESY spectra of free $_D$-*N,N,N*-trimethylglucosaminium (TMG)

Reference

1) H. Usuki, T. Nitoda, M. Ichikawa, N. Yamaji, T. Iwashita, H. Komura and H. Kanzaki, J. Am. Chem. Soc., 2008, 130, 4146-4152.

Section-7: Construction of ligand for docking simulations with *Sp*Hex.

A $GlcNAc_2$ unit was attached to the *twist-boat* form of TMG residue with β-1,4 linked manner followed by MMFF calculation to obtained the conformational structure (Fig. S13). The structure was used as the ligand for the docking simulation toward *Sp*Hex.

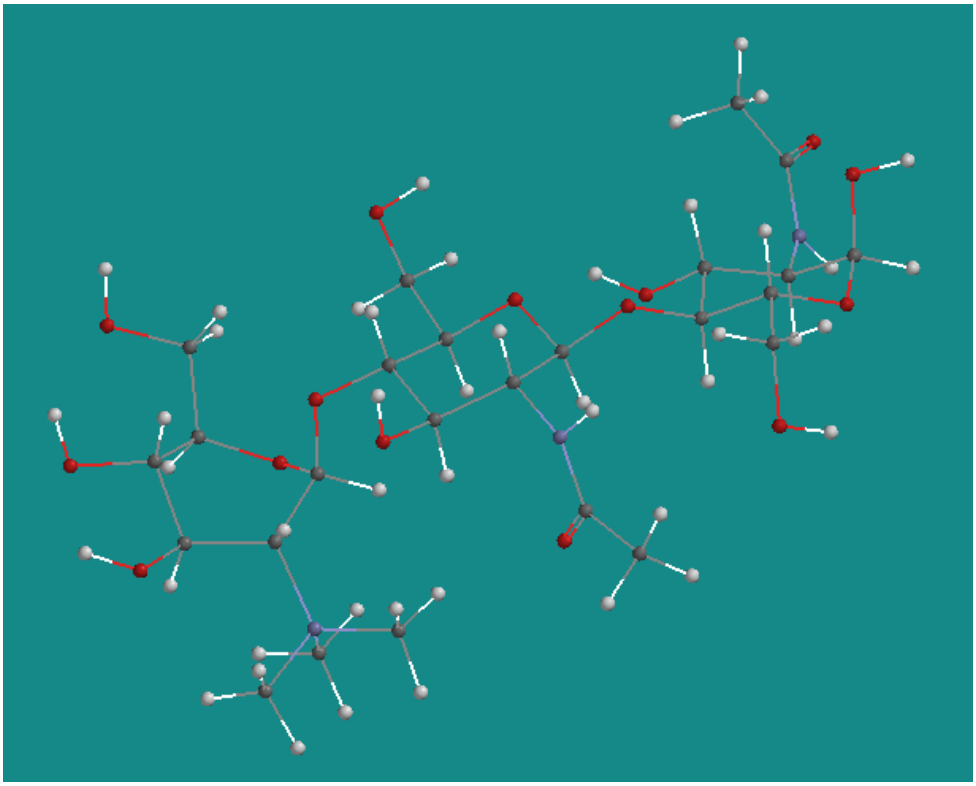

Fig. S13 Conformational structure of (2) as a ligand for the docking simulation

Section-8: Docking simulation between the TMG($^4C_1$ form)-chitobiomycin and *Sp*Hex.

TMG($^4C_1$ form)-chitobiomycin was constructed followed by the computational docking simulation toward *Sp*Hex. All of the procedures for this analysis were the same to that described in the main text. The result was shown in the Fig. S14. As shown in the figure, the TMG($^4C_1$ form)-chitobiomycin was predicted to be positioned at the surface of the protein, not the inside of the catalytic pocket. This result might indicate the essential effect of the *twist-boat* conformation of TMG to occupy the -1 subsite of the enzyme because the TMG(*twist-boat* form)-chitobiomycin was predicted to be positioned inside the catalytic pocket (see Fig. 7 of the main text).

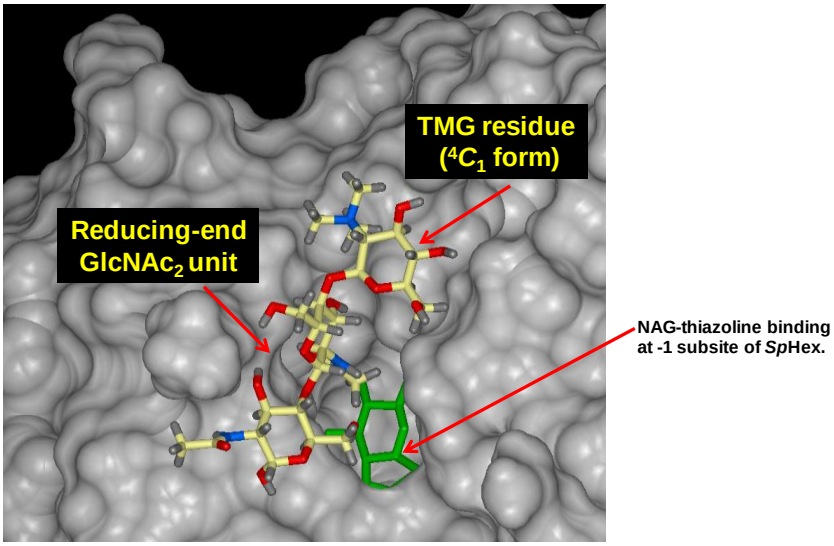

Fig. S14. Result of the docking simulation between the TMG($^4C_1$ form)-chitobiomycin and *Sp*Hex.

Section-9: UV absorption spectra of 2 and 3.

Compound **2** and **3** were dissolved in H_2O (**2**: 212 μM, **3**: 304 μM) followed by measuring their UV absorption spectra using the U 2800 Spectrometer (HITACHI). A quartz cell (l=1cm) was used for this analysis. As shown in Fig. S15, those of two compounds were quite a similar as expected by their chemical structures.

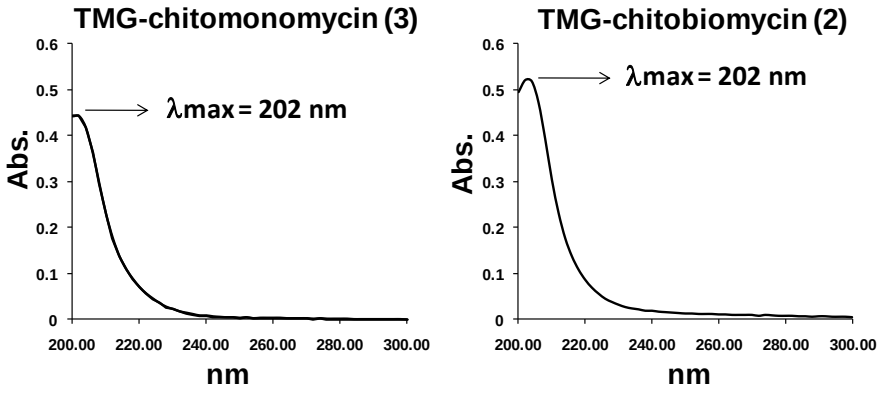

Fig. S15. UV absorption spectra of (2) and (3).